

The planting date experiment at Patancheru (Table 3) clearly showed that in early-maturity pigeonpea group, seed production of female parent and hybrid is possible at a single location. In this system the hybrid seed production plot must be sown in early rainy season (June); it will flower in about 60 days and all the flowers will be male-sterile. The cross-pollinated pods that would set on these plants can be harvested in another 40–45 days. However, for optimizing yields suitable agronomy packages need to be developed. The multiplication of female parent can be taken up in another isolation in September; the flowers produced on this crop will be fertile and a good harvest of female parent can be taken without the use of pollinating insects.

In crops where environment-sensitive gene(s) controlling male-sterility/fertility have been identified, the role of photo-period, temperature and their interaction is not well-defined. Future research on pigeonpea should now be concentrated on the issues such as identification of threshold temperature and photo-period at a given location that would control the function of fertility restoring system. Attempt should also be made to understand the molecular basis of sex reversion under different environments. Finally, it will be important to identify genes/quantitative trait loci responsible for controlling this trait that will facilitate quick transfer of these genes into heterotic hybrid parents.

1. Reddy, B. V. S., Green, J. M. and Bisen, S. S., Genetic male-sterility in pigeonpea. *Crop Sci.*, 1978, **18**, 362–364.
2. Saxena, K. B., Chauhan, Y. S., Johansen, C. and Singh, L., Recent advances in hybrid pigeonpea research. In *New Frontiers in Pulses Research and Development*, Directorate of Pulses Research, Kanpur, 1992, pp. 58–69.
3. Saxena, K. B., Kumar, R. V., Srivastava, N. and Shiyang, B., A cytoplasmic–nuclear male-sterility system derived from a cross between *Cajanus cajanifolius* and *C. cajan*. *Euphytica*, 2005, **145**, 291–296.
4. Saxena, K. B. *et al.*, ICPH 2671 – the world's first commercial food legume hybrid. *Plant Breed.*, 2013, **132**, 479–485.
5. Ariyanayagam, R. P., Rao, A. N. and Zaveri, P. P., Cytoplasmic–genic male-sterility in inter-specific matings of *Cajanus*. *Crop Sci.*, 1995, **35**, 981–985.
6. Saxena, K. B., Tikka, S. B. S. and Mazumdar, N. D., Cytoplasmic genic male-sterility in pigeonpea and its utilization in hybrid breeding programme. In *Pulses in New Perspective* (eds Ali, M., Singh, B. B., Kumar, S. and Dhar, V.), Indian Institute of Pulses Research, Kanpur, 2004, pp. 132–146.
7. Wallis, E. S., Byth, D. E. and Saxena, K. B., Flowering responses of thirty-seven early-maturing lines of pigeon pea. In Proceedings of the International Workshop on Pigeon Pea, 15–19 December 1980, ICRISAT, Patancheru, 1981, vol. 2, pp. 143–150.
8. Turnbull, L. V., Whiteman, P. C. and Byth, D. E., The influence of temperature and photoperiod on floral development of early flowering pigeon pea. In Proceedings of the International Workshop on Pigeon Pea, 15–19 December 1980, ICRISAT, Patancheru, 1981, vol. 1, pp. 217–223.
9. Saxena, K. B., Sultana, R., Mallikarjuna, N., Saxena, R. K., Kumar, R. V., Sawargonkar, S. L. and Varshney, R. K., Male-sterility systems in pigeonpea and their role in enhancing yield. *Plant Breed.*, 2010, **129**, 125–134.
10. Pring, D. R., Levings III, C. T., Hu, W. L. and Timonhy, D. H., Unique DNA associated with mitochondria in S cytoplasm of male sterile maize. *Proc. Natl. Acad. Sci. USA*, 1977, **74**, 2904–2908.
11. Escote, L. J., Susan, J. G. and John, R. L., Cytoplasmic reversion to fertility in CMS-S maize need not involve loss of linear mitochondrial plasmids. *Plasmid*, 1985, **14**, 264–267.
12. Sun, Z. X., Min, S. K. and Xiong, Z. M., A temperature sensitive male sterile line found in rice. *Rice Genet. Newsl.*, 1989, **6**, 116–117.
13. Maruyama, K., Araki, H. and Kato, H., Thermo-sensitive genetic male-sterility induced by radiation. In *Rice Genetics II*, International Rice Research Institute, Manila, 1991, pp. 227–232.
14. Zhang, Z. G., Yuan, S. C., Zen, H. L., Li, Y. Z. and Wang, X., Studies on fertility changes of photoperiod–temperature-sensitive genic male sterile W 6154s in response to temperature. *J. Huazhong Agric. Univ.*, 1991, **10**, 21–25.
15. Siddiq, E. A., Ahmad, I., Viraktamath, B. C., Ali, J. and Hoan, T., Status of hybrid rice research in India. In *Hybrid Research and Development* (eds Rai, M. and Mauria, S.), Indian Society of Seed Technology, New Delhi, 1995, pp. 139–158.
16. Dundas, I. S., Saxena, K. B. and Byth, D. E., Pollen mother cell and anther wall development in a photo-insensitive male sterile mutant in pigeonpea [*Cajanus cajan* (L.) Millsp.]. *Euphytica*, 1982, **31**, 309–313.
17. Kaul, M. L. H., *Male Sterility in Higher Plants*, Springer-Verlag, Berlin, 1988, p. 1805.
18. Tan, Z. C., Li, Y., Chen, L. B. and Zhou, G. Q., Studies on ecological adaptability of dual purpose line An-Nong S-1. *Hybrid Rice*, 1990, **3**, 35–38.

ACKNOWLEDGEMENTS. We thank Mr M. Satyanarayana (ICRISAT) for providing technical support while collecting data and Dr A. V. R. Kesava Rao (ICRISAT) for providing the weather data.

Received 12 December 2013; revised accepted 21 May 2014

Monitoring of glacier changes and response time in Chorabari Glacier, Central Himalaya, Garhwal, India

Manish Mehta*, D. P. Dobhal, Kapil Kesarwani, Bhanu Pratap, Amit Kumar and Akshya Verma

Centre for Glaciology, Wadia Institute of Himalayan Geology, Dehra Dun 248 001, India

Chorabari Glacier (6.6 sq. km) in the Mandakini River basin, a tributary of the River Alaknanda, Central Himalaya, Garhwal (India) has been monitored in terms of its length and frontal area (snout) changes for the period between 1962 and 2012. Global Positioning System, Survey of India toposheet (1 : 50,000) and ground-based measurements were used to obtain the changes in morphology and size of the glacier. The result shows that the frontal area of the glacier has

*For correspondence. (e-mail: msmehta75@gmail.com)

shrunk by 1% and 344 ± 24 m length loss, with an average rate of 6.8 ± 0.5 m a⁻¹ from 1962 to 2012. The observed terminus records of Chorabari Glacier indicate that the positive mass balance can cause terminus advance in about a 17-year timescale. The lag time of glacier signal transferred from accumulation area to the snout by glacier flow is about 562 years. These observations as well as other studies carried out in the region show a significant reduction in glacier area. The increased retreat rate of the glacier snout is probably a direct consequence of global warming.

Keywords: Frontal areas, glacier change, mass balance, response time, snout retreat.

MOST widely reported mountain glaciers are currently experiencing a period of recession, a trend that began in the mid-19th century with the end of the Little Ice Age^{1,2}. The rate of recession continued through the 20th century and has accelerated over the past three decades²⁻⁴. There is clear evidence that the retreat of glaciers in many locations of the world has accelerated in recent decades^{4,5}. However, glacier systems of the Himalaya have not responded uniformly to recent climate warming; some glaciers of western Karakoram Himalaya are advancing^{6,7}, while some glaciers of central and eastern Himalayas are retreating^{2,8}.

The Himalayan Mountain Range contains thousands of glaciers of widely varying properties, which are spread over nearly 37,000 sq. km and over a 2400 km east-west range⁹. This large geographical extent and complex topography along with the variable climatic conditions across the Himalayas has resulted in various sets of glacier properties. The primary climatic factor from west to east is that of a decreasing influence by the mid-latitude westerlies and an increasing influence by the Indian summer monsoon (ISM)¹⁰. Thus, the distribution of glaciers in the Himalaya is uneven, with a higher concentration of glaciers in the NW than in the NE of the mountain range. Glaciers located in the Central Himalaya are influenced both by the westerlies as well as ISM¹¹. In general, ~70% of the ablation zone of the glaciers is covered by debris with thickness ranging from millimetres to tens of centimetres^{1,9,12}. Due to the thick debris cover and with a low gradient of the termini, many glaciers typically have a stable front position. As a consequence of this complex climate system, glacial geometry and properties, and the geology, the recession rates of the glaciers are variable¹².

During the last few decades, the long-term monitoring of snout position and mass balance measurements have been carried out in several glaciers in different parts of the Indian Himalaya^{2,13-15}. The studies suggest that most of the glaciers are retreating between 5 and 20 m a⁻¹, with negative mass balance varying from 0.2 to 1.2 m a⁻¹ water equivalent^{13,14,16}. With such considerations and realizing of the potential significance of the glaciers and their recession process, *in situ* measurements of snout positions,

surface area changes and meteorological observations were carried out to quantify the total changes in the Chorabari Glacier, Central Himalaya, Garhwal, during the period 1962–2012.

The Chorabari Glacier (30°46'20.58"N, 79°2'59.381"E) is a medium-sized compound valley-type glacier covering an area of ~6.6 sq. km. It is located in the Mandakini River basin of the Alaknanda catchment (a tributary of the Ganga), Central Himalaya, Garhwal, India (Figure 1). The Chorabari Glacier has its accumulation area below Bhart Khunta peak (6578 m amsl) and Kedarnath peak (6940 m amsl) and flows from north to south between 6400 and 3895 m amsl, with an average surface slope of 20° (Figure 1). The accumulation area is comparatively small, steep and formed by three tributary glaciers, whereas the ablation area is broad with gentle slope and covered by thick debris. A number of longitudinal and transverse crevasses are prominent in the upper ablation zone and several small, supra-glacial lakes (ponds) are present in the glacier surface in the lower ablation zone. Debris thickness increases along the glacier, and is greater than >50 cm at the terminus (Figure 2). A second glacier (Companion) flows parallel to Chorabari. The traces of medial moraines (Figure 2) suggest that recession has separated the two glaciers. The extension of these lateral moraines is observed 6 km downstream at Rambara town (2800 m amsl). There appear to have been four stages of recession where traces of the lateral moraines are well preserved throughout the valley¹⁷. These glacier stages are Rambara Glacial Stage (RGS; 13 ± 2 ka), Ghindurpani Glacial Stage (GhGS; 9 ± 1 ka), Garuriya Glacial Stage (GGS; 7 ± 1 ka) and Kedarnath Glacial Stage (KGS; 5 ± 1 ka)¹⁷. During the 16 and 17 June 2013, very heavy rains together with breaching of moraine dammed Chorabari lake triggered flash floods that washed away all the glacial deposits in the down valley¹⁸. In summary, the characteristic features of this glacier are a south-facing, wide and broad terminus with thick debris covers. Some of the salient features of the glacier are given in Table 1.

The glaciers of the Himalayan region are not well documented because of inaccessibility of the area and poor meteorological and hydrological data. The monitoring of the Chorabari Glacier began in 2003. A manned meteorological observatory (3820 m amsl) was installed to monitor air temperature, wind speed and precipitation during the study period. The automatic weather station (AWS) (Campbell Instrument) was installed in 2007, near the snout of the glacier at an altitude of 3820 m amsl.

The general climate of the study area is humid-temperate in summer and dry-cold in winter¹⁹. The daily mean air temperature was observed near the snout of Chorabari Glacier at the height of 3820 m amsl for different seasons of 2007–2012. The average daily air temperature ranged from -13.46°C to 11.56°C , whereas the maximum and minimum air temperatures ranged from

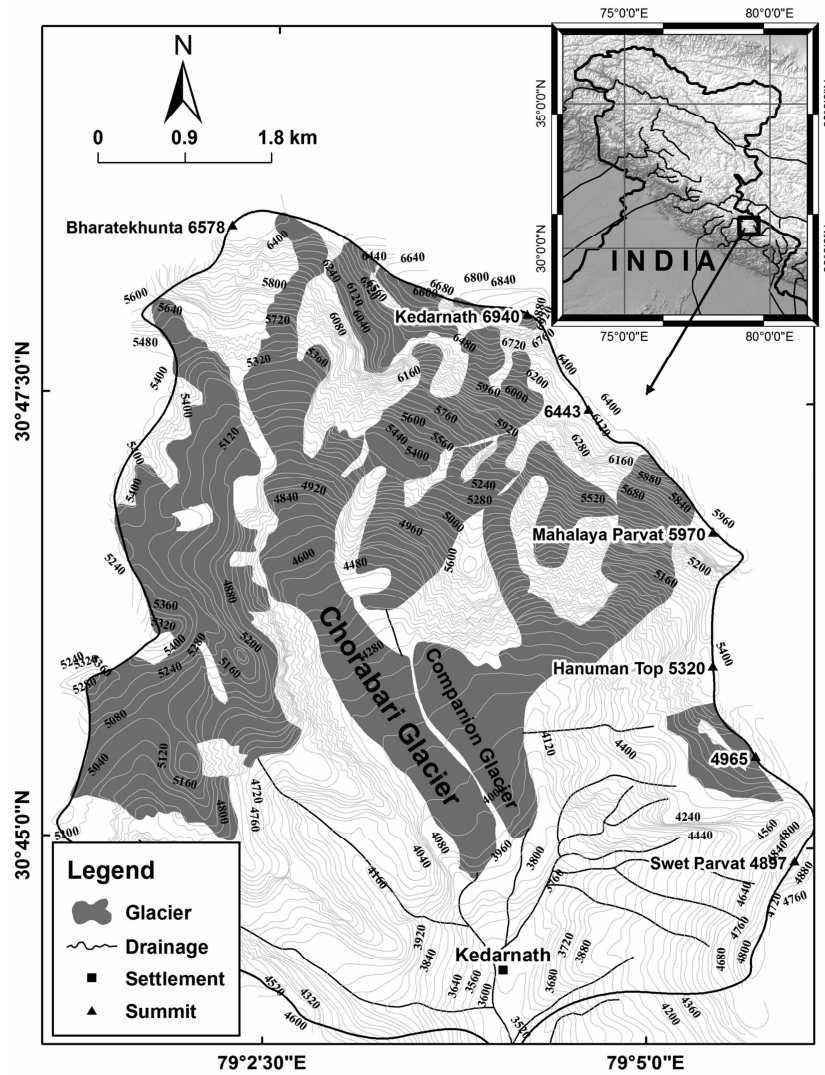


Figure 1. Location map of the study area. The shaded portion indicates the boundary of the Chorabari and other glaciers in the catchment area. (Source: Based on Survey of India toposheet 1962.)



Figure 2. Ground view of Chorabari and neighbouring glaciers that shows the past lateral extension and glaciation activities in the valley.

–9.39°C to 16.72°C and –19.5°C to 9.77°C respectively, between 2007 and 2012. During the study period the annual mean air temperature was ~3°C and average summer temperature (JJAS) was ~8.7°C. The maximum annual air temperature recorded was 16.7°C in June 2012 and the

minimum recorded was –19.5°C in February 2012. As usual, sudden drop in air temperatures was observed during rainfall and snowfall events in the study area.

Summer precipitation is highly influenced by the monsoon and average rainfall recorded between 2007 and

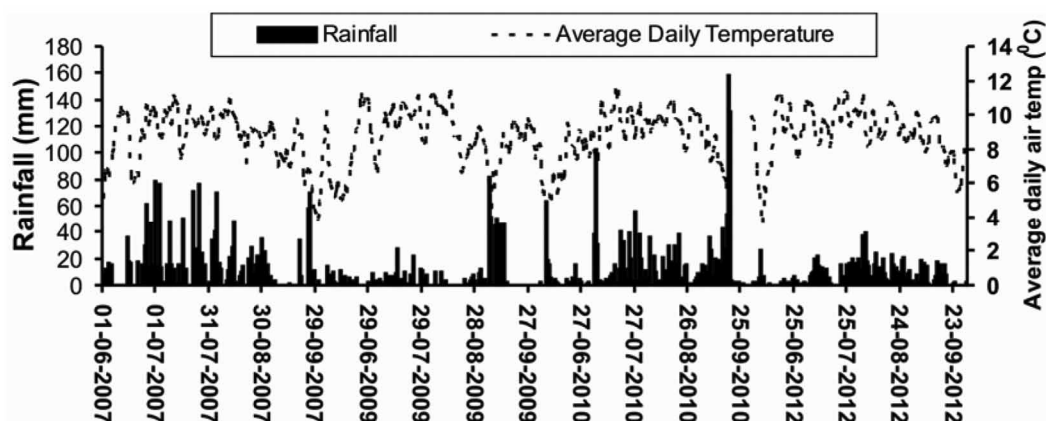


Figure 3. Temporal variation in daily precipitation (bar for left axis) and daily mean air temperature at Chorabari Glacier (3820 m amsl) during the summer (JJAS) period between 2007 and 2013.

Table 1. Salient features and geomorphological parameters of the Chorabari Glacier

Parameter	Chorabari Glacier
Coordinates	30°46'20.58"N, 79°2'59.381"E
Surface area (sq. km)	
1962	~7.37
2012	~6.66
Length (km)	~7.5 (2012)
Orientation	S
Elevation extension (m amsl)	3900–6420
Average surface slope (degree)	20
Mean width (km)	0.43
General climate	Humid–temperate in summer and dry–cold in winter
Average annual temperature at 3820 m amsl	3.39°C (2007–2010) Maximum (+) 16.72°C (June 2012) Minimum (–) 19.5°C (10 February 2012)
Geology (rock type)	Crystalline rocks, mainly augen and granitic gneisses

2012 was 1309 mm (June–October). Winter precipitation generally occurs between December and March when the westerlies are dominant in the area as they move eastward over northern India, and is the main source of snow accumulation. There are no instrumental data available for winter snowfall; however, residual snow depth fluctuated between 25 and 50 cm in April and early May at 4000 m amsl during the study period from 2003 to 2010 (ref. 20); snow normally melts before the commencement of the monsoon in mid-June. The average wind speed at AWS was 2.4 m s^{-1} and average daily sunshine duration was 190 min between 2007 and 2012. Summer (JJAS) daily means of the measured temperature and precipitation are shown in Figure 3.

The earliest record of Chorabari Glacier is available in the Survey of India topographic map (October 1962 edition) of 1 : 50,000 scale. In addition, the terminus (snout)

position was marked and the glacier was photographed in 1990 (ref. 20) and by remote sensing satellite images. The Chorabari Glacier is often heavily covered with supraglacial debris, making it difficult to study with remotely sensed images. Changes in the snout position were measured during the field seasons of 2003–2012 with handheld GPS (vertical accuracy (z) is $\pm 5 \text{ m}$ and horizontal accuracy (x, y) is $\pm 3 \text{ m}$), survey-grade total station measurements and field photographs. These data made it possible to identify the active ice margin of the debris-covered glacier, which was difficult to identify in satellite imagery. We have used Survey of India toposheet 1 : 50,000 scale with 40 m contour interval (planimetric accuracy $\pm 12.5 \text{ m}$ and elevation accuracy $\pm 6.5 \text{ m}$)²¹, Landsat ETM⁺ (1990; resolution 30 m) and ASTER (2007; resolution 15 m) images to map the glacier outline (Figure 4). The techniques and interpretation methodology follow those of Bhambri *et al.*⁸, Kulkarni *et al.*²² and Paul *et al.*²³. The glacier outline and frontal margin were measured by GPS and the annual position map of the glacier snout was prepared. Moreover, the glacier outline was verified by GPS survey on the side and frontal margins of the glacier and the annual position map of glacier snout was prepared. The area vacated by the glacier due to recession was estimated by superimposing an earlier survey map (1962) within a Geographical Information System (GIS). The methodology for monitoring the glacier snout positions and frontal area vacated was based on well-established techniques^{13,15,24,25}. Since 2003, the snout position and frontal area loss have been monitored by field survey. Three permanent reference stations were fixed near the frontal area of the glacier snout on stable ground (Figure 5). The geographical position of each reference station was determined by GPS and values obtained were transferred to the map. With the help of these fixed stable stations, the snout of Chorabari Glacier was mapped by GPS (fixed date measurements). To reduce the uncertainty and consistency of the changes

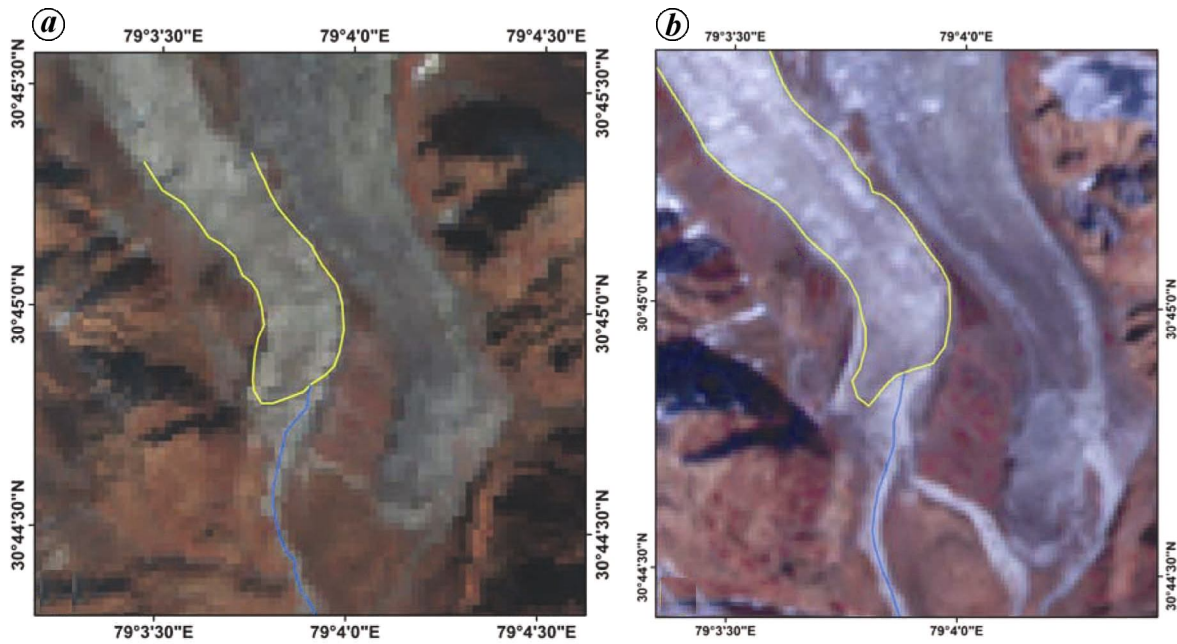


Figure 4. A successive recession trend showing the glacier boundary of Chorabari Glacier: *a*, Landsat ETM⁺ (1990; resolution 30 m); *b*, ASTER (2007; resolution 15 m) images to map the glacier outline.

in snout position, it is important to survey the glacier snout every year precisely as the retreat of the snout is not uniform. Accordingly, several point measurements were taken all around the terminus area as well as the centre and both sides of the glacier.

The error estimation for glacier length calculation was made from the total retreat from left, right and central parts of the snout. The total error (σ) was estimated as the root sum square of each error term. The error for glacier area was estimated by multiplication of uncertainty of length with glacial width.

It is essential to examine the terminus history of the glacier to calculate response time (T_m) and time lag (T_l) of the glacier. We use the following equations^{26–29} to calculate T_m and T_l for the Chorabari Glacier

$$T_m = h_t / -b_t, \quad (1)$$

$$T_l = fL / u_t, \quad (2)$$

where L is the glacier length; u_t the velocity of the glacier at the terminus, h_t the thickness of the glacier at the terminus and b_t is the net annual balance at the terminus. The component f is a valley shape factor, which is the ratio between thickness changes at the terminus and thickness changes at the glacier head^{27,28}. Equation (1) was proposed by Jóhannesson *et al.*²⁷ for the response times of 10 to 100 years and eq. (2) was proposed by Nye²⁶ for lag time or longer response times (100 to 1000 years). The changes in ice thickness will yield a value of $f=1$; $f=0.5$ corresponds to a linear decrease of thickness change from a maximum at the terminus to zero at the

head. The point mass balance data of Chorabari Glacier between 2003 and 2010 shows that the average ratio of thickness change between terminus and head of the glacier is ~ 0.28 (ref. 20). Here, we applied $f=0.28 \approx 0.3$ to determine the time lag (T_l) of Chorabari Glacier. Equation (2) is sensitive to terminus velocity, which is often spatially inconsistent²⁷.

The snout retreat of the Chorabari Glacier was measured. The Recession of the Chorabari Glacier between 1962 and 1990 was estimated to be 180 ± 8.5 m between 1962 and 1990 and 82 ± 6 m between 1990 and 2003 (ref. 20). Field measurements carried out from 2003 to 2012 show that the glacier had retreated 82 ± 9.2 m (Table 2). Based on the recession data, the annual retreat trends can be grouped into three time-intervals: (i) from 1962 to 1990 where the rate is estimated to be of the order of 6 ± 0.3 m a⁻¹; (ii) between 1990 and 2003 the calculated retreat rate is 6 ± 0.5 m a⁻¹ (ref. 20); (iii) field measurement between 2003 and 2012, when the retreat rate is calculated to be 9 ± 1 m a⁻¹ (Table 2). Thus it reveals that the present rate of retreat has increased slightly compared to previous periods (Figure 5 and Table 2). The cumulative reduction of 344 ± 24 m glacier length reveals that the Chorabari Glacier has lost $\sim 4\%$ of its total length during the last 50 years (1962 to 2012). The present snout position of the Chorabari Glacier is located at an altitude of 3895 m. During our observations, no advancement was recorded and the glacier showed a continuous recession trend (Figure 5).

The area vacated by the glacier in its pro-glacial region has been computed by comparing the historical maps with the present field measurements. The total frontal area

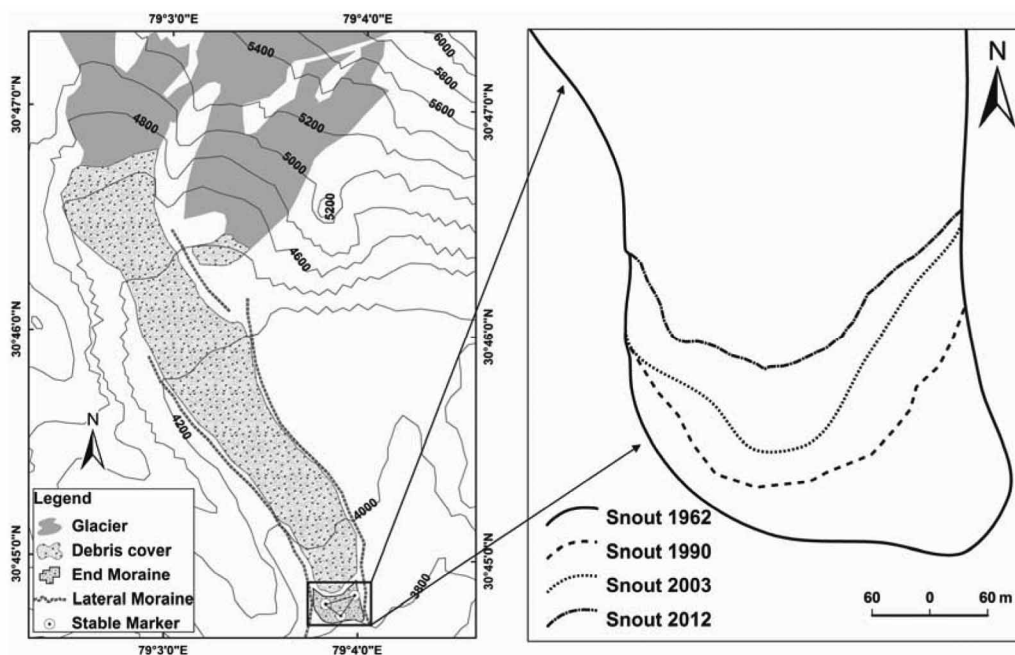


Figure 5. Surface morphological map of Chorabari Glacier along with stable survey marker (left) and snout retreat positions (right) during the period between 1962 and 2012.

Table 2. Snout recession of Chorabari Glacier during the period 1962–2012. Error (σ) comes from the total retreat from left, right and central parts of the snout

Period	No. of years	Recession (m)	Average recession (m a^{-1})
1962–1990	28	180 ± 8.5	6 ± 0.3
1990–2003	13	82 ± 6	6 ± 0.5
2003–2012	9	82 ± 9.2	9 ± 1
Total	50	344 ± 24	6.8 ± 0.5

Table 3. Total frontal area vacated by the Chorabari Glacier (1962–2012). The glacier lost ~1% frontal area between 1962 and 2012 (50 years)

Period	Years	Frontal area vacated (m^2)	Annual average ($\text{m}^2 \text{a}^{-1}$)
1962–2003	41	$58,490 \pm 3430$	1427 ± 84
2003–2007	4	$10,190 \pm 1949$	2548 ± 487
2007–2012	5	$9,049 \pm 1058$	3016 ± 353
Total loss	50	$77,729 \pm 6437$	1555 ± 129

vacated by the glacier for the period between 1962 and 2012 was $\sim 77,729 \pm 6437 \text{ m}^2$ with an average rate of $1555 \pm 129 \text{ m}^2 \text{ a}^{-1}$, which is approximately 1% of the total loss. During the period between 1962 and 2003, the glacier lost $58,490 \pm 3430 \text{ m}^2$ of its frontal area with an average of $1427 \pm 84 \text{ m}^2 \text{ a}^{-1}$ (ref. 19), while between 2003 and 2012 glacier recession increased and it lost

$19,239 \pm 3007 \text{ m}^2$ of its frontal area, with an average of $2138 \pm 334 \text{ m}^2 \text{ a}^{-1}$ (Table 3).

On the basis of these above-mentioned equations, we calculate T_m of the Chorabari Glacier; it is essential to examine the terminus history of the glacier. The terminus history of the 7.5 km long Chorabari Glacier has been determined for the period 1962 to 2012. It exhibits two distinct patterns: (i) slow retreat from 1962 to 1990, and (ii) slightly accelerated retreat from 1990 to 2012. The glacier showed continuous retreat and no advancement has been reported since 1962. During the periods between 2003 and 2010 (7 years), mass balance was calculated by Dobhal *et al.*¹⁹. The average net specific balance was -0.73 m water equivalent and average ablation at the terminus was -3.6 m (ref. 19). The average thickness of the glacier was $\sim 62 \text{ m}$ in the ablation zone and 10° slope at the terminus. Average velocity of the Chorabari Glacier at the terminus was $\sim 4 \text{ m a}^{-1}$ during the study period¹⁹.

The observed terminus records of Chorabari Glacier indicate that the positive mass balance can cause terminus advance in about a 17-year timescale. This is in rough agreement with the theory of Jóhannesson *et al.*²⁷, that suggest positive timescale between 10 and 100 years (eq. 1). The lag time of glacier signal transferred from accumulation area to the snout by glacier flow is about 562 years for the Chorabari Glacier. This time lag or response time comes from eq. (2) proposed by Nye²⁶ which produced longer response time or lag time of 100–1000 years.

The glacier surface change measured for more than 80 glaciers in Central western Himalaya suggested that most

of them are retreating since the end of the 19th century³⁰. Bhambri *et al.*³⁰ studied 82 glaciers in Alaknanda and Bhagirathi River basins in Central Himalaya using remote sensing data and archival records for the period 1968–2006, which showed 4.2% reduction in the glacierized area. The study also showed around 6% reduction associated with Alaknanda basin, and for 3% Bhagirathi basin. Similar observations were made in Chenab, Parbati and Baspa basins (466 glaciers) which showed overall 21% deglaciation from 1962 to 2001 (ref. 31). Satellite-based studies carried out on Millam Glacier in Goriganga basin between 1954 and 2006, showed that the glacier receded 1328 m with an average of $\sim 25 \text{ m a}^{-1}$ (ref. 32).

The scientific understanding of the glaciers of the Himalaya has been slow due to the complex topography and related lack of systematic or long-term field measurements though several studies have been done by remote sensing satellites. *In situ* measurements were made in the Dokriani Glacier (7 sq. km) in Garhwal Himalaya during 1962–2007, indicating the frontal area loss by the glacier to be $\sim 0.2\%$ (0.014 sq. km)³³. It is further observed that during this period the snout retreated by $\sim 680 \text{ m}$ with an average rate of $\sim 15 \text{ m a}^{-1}$. Regular monitoring of snout position of Dokriani Glacier was carried out annually on fixed datum (in October) for the period 1991–2007, which indicates fluctuation of the snout position ranging from $\sim 17.8 \text{ m a}^{-1}$ during 1991–2000 to 16.6 m a^{-1} during 2001–2007 (ref. 33). Similar observation has been reported from Tipra Glacier in Garhwal Himalaya during the period between 1962 and 2008. The study showed that the Tipra Glacier receded by $\sim 663 \text{ m}$ with an average of $\sim 14 \text{ m a}^{-1}$ and $\sim 4\%$ of frontal area was lost by the glacier during the same period¹⁵.

The above observations corroborate well with the study carried out in the Chorabari Glacier, where $262 \pm 14.5 \text{ m}$ recession ($6.4 \pm 0.4 \text{ m a}^{-1}$) during the period 1962–2003 and $82 \pm 9.2 \text{ m}$ ($9.1 \pm 1 \text{ m a}^{-1}$) in 2003–2012 was observed. The total $344 \pm 24 \text{ m}$ cumulative reduction of glacier length suggests that the Chorabari Glacier has lost $\sim 4\%$ ($0.08\% \text{ a}^{-1}$) of its total length during the last four decades. Overall, the glacier lost $\sim 77,729 \pm 6,437 \text{ m}^2$ of the frontal area between 1962 and 2012, which is $\sim 1\%$ of the total glacier area. However, terminus records of Chorabari Glacier indicate that the positive mass balance can cause terminus advance in about a 17-year timescale. The lag time (T_l) of the glacier signal transferred from accumulation area to the snout by glacier flow is about 562 years. In comparison with the other glaciers of Central western Himalaya, the Chorabari Glacier is receding at a very slow rate, which may be attributed to the local factors controlling the behaviour of these glaciers. These include differences in local climatic history and/or differences in intrinsic sensitivity of the glacier to climate change as a result of differences in geometry, bedrock slope, orientation, elevation, rate of mass turnover and thickness of the debris of the glacier. The Chorabari Gla-

acier has thick debris-covered ablation area, with debris thickness ranging from millimetres to tens of centimetres. Debris thickness increases along the glacier, and is thicker than $>50 \text{ cm}$ at the terminus of the glacier. Supraglacial debris commonly found on glaciers has significant control on the rate of ice ablation^{34,35}.

The recent trends of air temperature are varying across the region. In central/eastern Himalaya, Shrestha *et al.*³⁶ reported increasing temperature trends ranging from $0.06^\circ\text{C a}^{-1}$ to $0.12^\circ\text{C a}^{-1}$ in most of the regions of the Nepal Himalaya. Bhutiyani *et al.*³⁷ reported a significant rise in air temperature in the north-western Himalaya in the last century. An increase in maximum and minimum temperatures by $\sim 1^\circ\text{C}$ and $\sim 3.4^\circ\text{C}$ respectively, was found across the Great Himalayan region during the period between 1988 and 2008 (ref. 38). The increase in temperature was accompanied by decreasing trends in precipitation, and a reduction in total seasonal snowfall^{38,39}. In contrast, the Karakoram Range experienced a decreasing trend in maximum and minimum temperatures of 1.6°C and 3.0°C respectively³⁸, together with an increase in winter precipitation⁴⁰.

The glacier accumulation and ablation patterns are distinctly different, seasonally and spatially, across the region. In the east, the summer season typically includes both maximum accumulation and maximum melt (accumulation at the highest elevations with melt below), whereas in the west there is a general pattern of summer melt and winter accumulation. Glacier termini extend to lower elevations, approximately 2500 m, in the west, compared to approximately 3500–4500 m in the east/centre, due primarily to the lower temperatures at the higher latitudes of the more western mountain ranges¹¹.

The studies carried out during the last century provide a link between climate change and glacier retreat^{41,42}. Enhanced retreating rates have been observed in the eastern and central parts of the Himalaya^{8,15,21,22,43}. In the north-western Himalaya, an expansion and thickening of the larger glaciers has been reported, specially in the Karakoram since the 1990s, accompanied by an exceptional number of glacier surges^{2,6,44–46}. Other studies based on multi-sensor remote sensing analysis and gravity data from the Gravity Recovery and Climate Experiment (GRACE) reported positive mass balance anomalies in the Karakoram for the same period^{46,47}.

In this study we have presented the results of the frontal area and length loss of the Chorabari Glacier between 1962 and 2012. The glacier is continuously retreating and no advancement has been reported since 1962. The glacier has lost $\sim 1\%$ of its frontal area and $\sim 344 \text{ m}$ of its length since 1962. Between 1962 and 2003, the glacier lost about 262 m length with an average rate of 6 m a^{-1} and lost $\sim 0.055 \text{ sq. km}$ area with an average of $\sim 0.0013 \text{ km a}^{-1}$. Ground-based measurement shows that the glacier lost $\sim 82 \text{ m}$ length and 0.02 sq. km area, with an average rate of 9 m a^{-1} and $0.002 \text{ sq. km a}^{-1}$ respectively, between

2003 and 2012. Terminus records indicate that the positive mass balance can cause terminus advance in about 17-year timescale. Lag time of glacier signal transferred from accumulation area to snout by glacier flow is about 562 years. This trend of glacier reduction is similar to those observed in Central western Himalaya. The reduction is not only caused by temperature, but also by precipitation and terminus dynamics. Moreover, the rate of recession of Chorabari Glacier is slow compared to other glaciers, which can be explained by the topography and the effect of debris thickness.

1. Kamp, U., Byrne, M. and Bolch, T., Glacier fluctuations between 1975 and 2008 in the Greater Himalaya Range of Zaskar, southern Ladakh. *J. Mt. Sci.*, 2011, **8**, 374–389; DOI:10.1007/s11629-011-2007-9.
2. Bolch, T. *et al.*, The State and fate of Himalayan glaciers. *Science*, 2012, **336**(6079), 310–314; DOI:10.1126/science.1215828.
3. Barry, R., The status of research on glaciers and global glacier recession: a review. *Prog. Phys. Geogr.*, 2006, **30**, 285–306; DOI:10.1191/0309133306.
4. Zemp, M., Roer, I., Kääb, A., Hoelzle, M., Paul, F. and Haerberli, W., Global glacier changes: facts and figures. World Glacier Monitoring Service, United Nations Environment Programme, Geneva, 2008, p. 80.
5. Cogley, J. G., Present and future states of Himalaya and Karakoram glaciers. *Ann. Glaciol.*, 2011, **52**(59), 69–73.
6. Hewitt, K., The Karakoram anomaly? Glacier expansion and the elevation effect, Karakoram Himalaya. *Mt. Res. Dev.*, 2005, **25**, 332–340.
7. Gardelle, J., Berthier, E. and Arnaud, Y., Slight mass gain of Karakoram glaciers in the early twenty-first century. *Nature Geosci.*, 2012, **5**, 322–325; DOI:10.1038/ngeo1450.
8. Bhambri, R., Bolch, T. and Chaujar, R. K., Frontal recession of Gangotri Glacier, Garhwal Himalayas from 1965 to 2006, measured through high-resolution remote sensing data. *Curr. Sci.*, 2012, **102**(3), 489–494.
9. Raina, V. K. and Srivastava, P., *Glacier Atlas of India*, Geological Society of India, Bangalore, 2008.
10. Bookhagen, B. and Burbank, D. W., Towards a complete Himalayan hydrologic budget: the spatiotemporal distribution of snow melt and rainfall and their impact on river discharge. *J. Geophys. Res.*, 2010, **115**, F03019; DOI:10.1029/2009JF001426.
11. Armstrong, R. L., The glaciers of the Hindu Kush–Himalayan region – a summary of the science regarding glacier melt/retreat in the Himalayan, Hindu Kush, Karakoram, Pamir, and Tien Shan mountain ranges. ICIMOD, Kathmandu, Nepal, 2011, p. 17.
12. Scherler, D., Bookhagen, B. and Strecker, M. R., Spatially variable response of Himalayan glaciers to climate change affected by debris cover. *Nature Geosci.*, 2011, **4**, 156–159; DOI:10.1038/ngeo1068.
13. Wagnon, P. *et al.*, Four years of mass balance on Chhota Shigri Glacier, Himachal Pradesh, India, a new benchmark glacier in the western Himalaya. *J. Glaciol.*, 2007, **53**, 603–611; DOI:10.3189/002214307784409306.
14. Dobhal, D. P., Gergan, J. T. and Thayyen, R. J., Mass balance studies of the Dokriani Glacier from 1992 to 2000, Garhwal Himalaya, India. *Bull. Glaciol. Res.*, 2008, **25**, 9–17.
15. Mehta, M., Dobhal, D. P. and Bhist, M. P. S., Change of Tipra Glacier in the Garhwal Himalaya, India, between 1962 and 2008. *Prog. Phys. Geogr.*, 2011, **35**(6), 721–738.
16. Kulkarni, A. V., Mass balance of Himalayan glaciers using AAR and ELA methods. *J. Glaciol.*, 1992, **38**(128), 101–104.
17. Mehta, M., Majeed, Z., Dobhal, D. P. and Srivastava, P., Geomorphological evidences of post-LGM glacial advancements in the Himalaya: a study from Chorabari Glacier, Garhwal Himalaya, India. *J. Earth Syst. Sci.*, 2012, **121**(1), 149–163.
18. Dobhal, D. P., Gupta, A. K., Mehta, M. and Khandelwal, D. D., Kedarnath disaster: facts and plausible causes. *Curr. Sci.*, 2013, **105**(2), 171–174.
19. Dobhal, D. P., Mehta, M. and Srivastava, D., Influence of debris cover on terminus retreat and mass changes of Chorabari Glacier, Garhwal region, central Himalaya, India. *J. Glaciol.*, 2013, **59**(217), 961–971.
20. Gergan, J. T., Dobhal, D. P. and Chaujar, R., Technical report on reconnaissance survey of glaciers in Garhwal Himalaya, WIHG, Dehradun, 1990, No. 33.
21. Prasada Raju, P. V. S. P. and Ghosh, S., Role of remote sensing and digital cartography in sustainable development. In *Indian Cartography*, 2003, pp. 88–95.
22. Kulkarni, A. V., Bahuguna, I. M., Rathore, B. P., Singh, S. K., Randhawa, S. S., Sood, R. K. and Dhar, S., Glacial retreat in Himalaya using Indian remote sensing satellite data. *Curr. Sci.*, 2007, **92**(1), 69–74.
23. Paul, F., Huggel, C. and Kääb, A., Combining satellite multi spectral image data and a digital elevation model for mapping debris-covered glaciers. *Remote Sensing Environ.*, 2004, **89**(4), 510–518.
24. Østrem, G. and Brugman, M., *Glacier Mass Balance Measurements: A Manual for Field and Office Work*, National Hydrology Research Institute, Saskatoon, Canada, and the Norwegian Water Resources and Electricity Board, Oslo, Norway, 1991.
25. Dobhal, D. P., Gergan, J. T. and Thayyen, R. J., Recession and morphogeometrical changes of Dokriani glacier (1962–1995), Garhwal Himalaya, India. *Curr. Sci.*, 2004, **86**(5), 692–696.
26. Nye, J. F., The response of glaciers and ice-sheets to seasonal and climate changes. *Proc. R. Soc. London, Ser. A*, 1960, **256**(1287), 559–584.
27. Jóhannesson, T., Raymond, C. and Waddington, E., Time-scale for adjustment of glaciers to changes in mass balance. *J. Glaciol.*, 1960, **35**, 355–369.
28. Paterson, W. S. B., *Physics of Glaciers*, Pergamon Press, Oxford, UK, 1994, 3rd edn.
29. Pelto, M. S. and Hedlund, C., The terminus behavior and response time of North Cascade glaciers. *J. Glaciol.*, 2001, **47**, 497–506.
30. Bhambri, R., Bolch, T., Chaujar, R. K. and Kulshreshtha, S. C., Glacier changes in the Garhwal Himalayas, India 1968–2006 based on remote sensing. *J. Glaciol.*, 2011, **57**(203), 543–556.
31. Kulkarni, A. V., Rathore, B. P., Mahajan, S. and Mathur, P., Alarming retreat of Parbati Glacier, Beas basin, Himachal Pradesh. *Curr. Sci.*, 2005, **88**(11), 1844–1850.
32. Babu, K. B. G., Recession and reconstruction of Milam Glacier, Kumaon Himalaya, observed with satellite imagery. *Curr. Sci.*, 2011, **100**(9), 1420–1425.
33. Dobhal, D. P. and Mehta, M., Surface morphology, elevation changes and terminus retreat of Dokriani Glacier, Garhwal Himalaya: implication for climate change. *Him. Geol.*, 2010, **31**(1), 71–78.
34. Bozhinskiy, A. N., Krass, M. S. and Popovnin, V. V., Role of debris cover in the thermal physics of glaciers. *J. Glaciol.*, 1986, **32**(111), 255–266.
35. Lundstrom, S. C., McCafferty, A. E. and Coe, J. A., Photogrammetric analysis of 1984–89 surface altitude change of the partially debris-covered Eliot Glacier, Mount Hood, Oregon, USA. *Ann. Glaciol.*, 1993, **17**, 167–170.
36. Shrestha, A. B., Wake, C. P., Mayewski, P. A. and Dibb, J. E., Maximum temperature trends in the Himalaya and its vicinity: an analysis based on temperature records from Nepal for the period 1971–94. *J. Climate*, 1999, **12**, 2775–2767.
37. Bhutiyan, M. R., Vishwas, S. K. and Pawar, N. J., Long-term trends in maximum, minimum and mean annual air temperatures

across the Northwestern Himalaya during the twentieth century. *Climate Change*, 2007, **85**, 159–177; DOI:10.1007/s10584-006-9196-1.

38. Shekhar, M. S., Chand, H., Kumar, S., Srinivasan, K. and Ganju, A., Climate change studies in the western Himalaya. *Ann. Glaciol.*, 2010, **51**(54), 105–112; DOI:10.3189/172756410791386508.
39. Dimri, A. P. and Kumar, A., Climatic variability of weather parameters over the western Himalayas: a case study. In Proceedings of the National Snow Science Workshop, Chandigarh, Snow and Avalanche Study Establishment, 11–12 January 2008.
40. Fowler, H. J. and Archer, D. R. Conflicting signals of climate change in the upper Indus basin. *J. Climate*, 2006, **19**(17), 4276–4293; DOI:10.1175/JCLI3860.1.
41. Haeblerli, W., Zemp, M., Frauenfelder, R., Hoelzle, M. and Kaab, A., *Fluctuations of Glaciers 1995–2000, Volume 8*, UNESCO, World Glacier Monitoring Service, Zurich, Switzerland, 2005, p. 288.
42. Kaser, G., Cogley, J. G., Dyurgerov, M. B., Meier, M. F. and Ohmura, A., Mass balance of glaciers and ice caps: consensus estimates for 1961–2004. *Geophys. Res. Lett.*, 2006, **33**, 1–5; DOI: 10.1029/2006GL027511.
43. Bajracharya, S. R., Mool, P. K. and Shrestha, B. R., Impact of climate change on Himalayan glaciers and glacial lakes: case studies on GLOF and associated hazards in Nepal and Bhutan, ICIMOD, Kathmandu, 2007, p. 119.
44. Immerzeel, W. W., Droogers, P., De Jong, S. M. and Bierkens, M. F. P., Large-scale monitoring of snow cover and runoff simulation in Himalayan river basins using remote sensing. *Remote Sensing Environ.*, 2009, **113**, 40–49; DOI:10.1016/j.rse.2008.08.010.
45. Quincey, D. J., Braun, M., Glasser, N. F., Bishop, M. P., Hewitt, K. and Luckman, A., Karakoram glacier surge dynamics. *Geophys. Res. Lett.*, 2011, **38**, L18504; DOI:10.1029/2011GL049004.
46. Jacob, T., Wahr, J., Pfeffer, W. T. and Swenson, S., Recent contributions of glaciers and ice caps to sea level rise. *Nature*, 2012, **482**, 514–518; DOI:10.1038/nature10847.
47. Bishop, M. P. *et al.*, Advancing glaciers and positive mass anomaly in the Karakoram Himalaya, Pakistan. In Paper presented at the American Geophysical Union Fall Meeting, San Francisco, USA, 15–19 December 2008.

ACKNOWLEDGEMENTS. We thank the Director, Wadia Institute of Himalayan Geology (WIHG), Dehra Dun, for providing the necessary facilities. We also thank Sri Deepak Srivastava (Consultant) for discussions and valuable suggestions; Dr Rakesh Bhambri and Dr Indra Karakoti (WIHG) for help during manuscript preparation and the Department of Science and Technology, New Delhi for financial support.

Received 7 November 2013; revised accepted 18 May 2014

Thermal performance of a low-concentration ethanol stove without pressure system

Andrianantenaina Marcelin Hajamalala*

Laboratory of Applied Physics of the University of Fianarantsoa, Madagascar

We report here the thermal performance of a new burner running on low-concentration ethanol (50°GL) without pressure system. The experimental method based on the water boiling point of water developed by Shell Foundation, consists of three phases of test used to study the performance of the stove. Test and calculation results show that the time to boil 2.5 l of water is 19.6 min in cold start and 18.4 min in hot start. The specific consumption is 25.55 g/l for the boiling task and 29.4 g/l for the simmering task. The thermal efficiency calculation of the stove is 55.75% in high power and 58.3% in simmer with a turndown ratio of 2.24. The average thermal output of the stove is from a high of 1575 W to a low of 694 W. The optimal thermal output is 694 W, with a thermal efficiency of 59%. The results show that the burner can transform gradually the low ethanol–water mixture of 50% (w/w) to a vapour of ethanol–water mixture concentration of 68.55% (w/w) in cold start, 73.71% (w/w) in hot start and 68.47% (w/w) in simmer. Improving the nature of the burner components helps improve the performance of the stove and also has an impact on its lifespan. The performance of the stove depends on the variation of the concentration of ethanol fuel during the test. The experimental study showed that the stove running on 50% v/v ethanol–water mixture is a no smoking stove, with no danger of fires.

Keywords: Burner, ethanol stove, thermal efficiency, water boiling test.

MALAGASY forest resources have been in a state of regression for several decades. The principal causes of deforestation are land clearance for agriculture, wild fires, fuelwood use for household energy, wood for construction and wood fuel for energy¹. Forest cover constitutes less than 25% of the total land area of Madagascar. The country has already lost 80% of its natural area, and continues to lose an estimated 200,000 ha annually to deforestation. If the rate of forest reduction remains at the current level, i.e. 0.55% per annum, all of Madagascar's forests will be lost within 40 years². In this context careful zoning and planning of agricultural encroachment into new areas would have to be integrated into a policy aimed at expanding sugarcane ethanol production in Madagascar

*e-mail: hajamalalaa@yahoo.fr